High-efficiency cascaded wavelength conversion based on adiabatic evolution

Junxiong Wei, Changshui Chen,* He Jiang, Wei Li, and Tian Han
Laboratory of Nanophotonic Functional Materials and Devices and MOE Key Laboratory of Laser Life Science & Institute of Laser Life Science, South China Normal University, Guangzhou, Guangdong 510631, China
(Received 16 April 2013; published 5 August 2013)

We demonstrate that the frequency conversion in the cascaded processes can be mapped uniquely to an associated three-wave mixing processes in adiabatic evolution. After solving the coupling wave equations of three-wave mixing processes, we immediately find the solutions of the corresponding cascaded coupled equations. Furthermore, we introduce a rather simple model, which displays the main features of the optical stimulated Raman adiabatic passage (STIRAP) but allows for analytic evaluation of all quantities. It performs two simultaneous three-wave mixing processes efficiently and without significant generation of an intermediate frequency. At last, we consider in detail the effects of the phase mismatch to the optical STIRAP efficiency, which show that the analytic bounds are seen to describe the transfer region very accurately.

DOI: 10.1103/PhysRevA.88.023806 PACS number(s): 42.65.Ky

I. INTRODUCTION

Mid-infrared lasers in the 3 to 5 μm wavelength region have many applications, such as military countermeasures and remote monitors of the special environment, spectrum, and so on [1,2]. Combined with quasi-phase matching (QPM) and based on optical parametric oscillators (OPO) [3] or difference frequency generation (DFG) [4], nonlinear optical frequency conversion can effectively produce an infrared source. However, recent advances in quasi-phase-matching (QPM) technology, which is based on periodically poled nonlinear crystals, have motivated great interest in the physics and applications of multistep optical parametric processes [5–7]. By using an analogy to stimulated Raman adiabatic passage (STIRAP) in atomic physics [8], Porat *et al.* [9,10] proposed a scheme in which the input frequency (ω_1) is directly converted into an output frequency (ω_4) without significant generation of the intermediate frequency (ω_3). A unique feature of optical STIRAP is that the intermediate frequency ω_3 will never generate. The reason is that throughout the adiabatic evolution the multistep parametric processes remain trapped in a dark vector, $C_0(z)$, which is only a superposition of the frequencies ω_1 and ω_4 and does not involve the intermediate frequency ω_3. If the modulations' order is counterintuitive, then the dark vector is initially associated with frequency ω_1 and finally with frequency ω_4, thus providing an adiabatic route from ω_1 to ω_4. Because the existence of the dark vector $C_0(z)$ is vital for optical STIRAP, and utilization of the adiabatic elimination procedure can also directly generate frequency ω_4, maintaining the perfect phase matching is usually considered crucial for optical STIRAP. This is indeed correct when the pump and Stokes couplings possess approximately equal peak values, which is favorable for optical STIRAP and which is also the assumption stated in Ref. [10].

In this paper, we introduce a model which displays the main features of the optical STIRAP situation but allows analytic evaluation of all quantities. It is based on the fact that the cascaded conversion processes can be mapped uniquely to an associated three-wave mixing processes. We formulate a general result and introduce the analytic approximations from the adiabatic theory of three-wave mixing processes. This could provide us with the solution to a nontrivial case of the STIRAP process in the adiabatic frequency conversion situation. Moreover, the sensitivity of the optical STIRAP to phase mismatch has been analyzed. The method is suggested in Ref. [11], in which the STIRAP technique is a function of the two-photon detuning. By analyzing the emerged adiabatic basis crossings and the positions of the nonadiabatic couplings, we are able to derive accurate bounds of the efficient frequency conversion region and estimate the width of the phase mismatching. Finally, a technologically feasible method for carrying out such a process is proposed and numerically demonstrated to be effective.

II. DYNAMICAL EQUATIONS

We consider two simultaneous three-wave mixing (STWM) processes, as shown in Fig. 1. The two simultaneous DFG processes are simultaneously realized in a single super lattice.

Under the plane-wave approximation and considering the QPM condition, the coupling equations for the dimensionless field amplitudes ψ_j which describe the cascaded interactions are as follows:

$$\frac{d}{dz}\psi_1 = \frac{-i\omega_1 d_{\text{eff}}}{n_1 c} f_1\psi_2\psi_3 e^{i\Delta k_1 z}, \tag{2.1a}$$

$$\frac{d}{dz}\psi_2 = \frac{-i\omega_2 d_{\text{eff}}}{n_2 c}(f_1\psi_1\psi_3^* e^{-i\Delta k_1 z} + f_2\psi_3\psi_4 e^{i\Delta k_2 z}), \tag{2.1b}$$

$$\frac{d}{dz}\psi_3 = \frac{-i\omega_3 d_{\text{eff}}}{n_3 c}(f_1\psi_1\psi_2^* e^{-i\Delta k_1 z} + f_2\psi_2\psi_4^* e^{-i\Delta k_2 z}), \tag{2.1c}$$

$$\frac{d}{dz}\psi_4 = \frac{-i\omega_4 d_{\text{eff}}}{n_4 c} f_2\psi_2\psi_3^* e^{-i\Delta k_2 z}, \tag{2.1d}$$

where z is the position along the propagation axis. Difference frequency $\omega_3 = \omega_1 - \omega_2$ and difference frequency $\omega_4 = \omega_2 - \omega_3$. The electric field at frequency ω is $E = \sqrt{P_0^\omega/2\varepsilon_0 cn}\psi(z)\exp(i\omega t - ikz) + \text{c.c.}$, where P_0^ω is the input power of the frequency ω field. c is the speed of light

*Corresponding author: cschen@aiofm.ac.cn

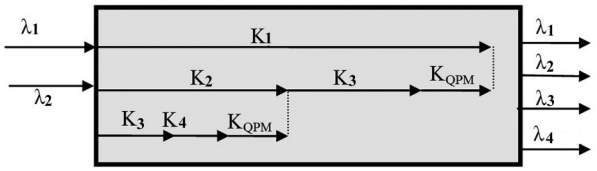

FIG. 1. Schematic illustration of cascaded difference frequency generation process.

in vacuum, f_1 and f_2 are the magnitudes of the Fourier coefficients, and d_{eff} is the second-order nonlinear coefficient. n_j is the refractive index and the phase mismatches are Δk:

$$\Delta k_1 = n_2\omega_2/c + n_3\omega_3/c - n_1\omega_1/c + 2\pi/\Lambda_1,$$
$$\Delta k_2 = n_3\omega_3/c + n_4\omega_4/c - n_2\omega_2/c + 2\pi/\Lambda_2.$$

Undepleted pump approximation. The undepleted pump approximation is when the incident signal field E_2 is much stronger than the other fields and therefore its amplitude is nearly constant (undepleted) during the evolution. So the coupled equations that govern the evolution of the two STWM processes can be written in three linear equations [10]:

$$i\frac{d}{dz}\varphi(z) = M(z)\varphi(z), \quad M(z) = \begin{bmatrix} \Delta k_1 & \Omega_p^* & 0 \\ \Omega_p & 0 & \Omega_s^* \\ 0 & \Omega_s & -\Delta k_2 \end{bmatrix}, \tag{2.2}$$

$$\varphi(z) = [\varphi_1,\varphi_2,\varphi_3]^T, \quad \Omega_p = \psi_2\sqrt{g_1 g_{31}}, \quad \Omega_s = \psi_2\sqrt{g_4 g_{32}},$$
$$\varphi_1(z) = \psi_1(z)\psi_2(z)e^{-i\Delta k_1 z}\sqrt{g_{31}g_4/2},$$
$$\varphi_2(z) = \psi_2(z)\psi_3(z)\sqrt{g_1 g_4/2},$$
$$\varphi_3(z) = \psi_2(z)\psi_4(z)e^{-i\Delta k_2 z}\sqrt{g_1 g_{32}/2}.$$

Here $g_1 = \frac{-i\omega_1 d_{\text{eff}}}{n_1 c} f_1$, $g_{31} = \frac{-i\omega_3 d_{\text{eff}}}{n_3 c} f_1$, $g_{32} = \frac{-i\omega_3 d_{\text{eff}}}{n_3 c} f_2$, and $g_4 = \frac{-i\omega_4 d_{\text{eff}}}{n_4 c} f_2$. Equations (2.2) have the same form as the dynamics of the quantum mechanical three-level Λ system. The off-diagonal elements Ω_p and Ω_s provide couplings between the optical fields, which correspond to the pump and Stokes Rabi frequencies of the three-level Λ system, both of which are proportional to the signal field E_2 and the magnitudes of the Fourier coefficients.

It is convenient to single out the phase mismatch terms of matrix $M(z)$ by dividing it into two parts:

$$M(z) = M_0(z) + M_\Delta(z), \quad M_0(z) = \begin{bmatrix} 0 & \Omega_p^* & 0 \\ \Omega_p & 0 & \Omega_s^* \\ 0 & \Omega_s & 0 \end{bmatrix},$$
$$M_\Delta(z) = \begin{bmatrix} \Delta k_1 & 0 & 0 \\ 0 & 0 & 0 \\ 0 & 0 & -\Delta k_2 \end{bmatrix}, \tag{2.3}$$

where the matrix $M_0(z)$ corresponds to the usual STIRAP Hamiltonian $H_0(t)$, and $M_\Delta(z)$ accounts for the two-photon detuning δ. We suppose that at $z = 0$ the optical field is $\varphi_1(z = 0) = 1$, $\varphi_2(z = 0) = 0$, and $\varphi_3(z = 0) = 0$, and we are interested in the power at $z = L$ (crystal length) and $P_n(z = L) = |\varphi_n(z = L)|^2$ ($n = 1$, 2, and 3).

We first consider the case of perfect phase matching $\Delta k_1 = \Delta k_2 = 0$. The eigenvalues of matrix $M(z)$ are

$$\varepsilon_0(z) = 0, \quad \varepsilon_+(z) = \sqrt{\Omega_p^2 + \Omega_s^2}, \quad \varepsilon_-(z) = -\sqrt{\Omega_p^2 + \Omega_s^2}. \tag{2.4}$$

The corresponding eigenvectors of $M(z)$ that form the adiabatic basis are

$$\lambda_0 = [-\Omega_s^*, 0, \Omega_p]^T, \quad \lambda_+ = \left[\Omega_p^*, -\sqrt{\Omega_p^2 + \Omega_s^2}, \Omega_s\right]^T,$$
$$\lambda_- = \left[\Omega_p^*, \sqrt{\Omega_p^2 + \Omega_s^2}, \Omega_s\right]^T. \tag{2.5}$$

Next, let us define the mixing angle θ: $\tan\theta(z) = \Omega_p/\Omega_s$; then the adiabatic basis is as follows:

$$C_+(Z) = \frac{\sin\theta}{\sqrt{2}}\varphi_1(Z) - \frac{1}{\sqrt{2}}\varphi_2(Z) + \frac{\cos\theta}{\sqrt{2}}\varphi_3(Z), \tag{2.6a}$$
$$C_0(Z) = \cos\theta\varphi_1(Z) - \sin\theta\varphi_3(Z), \tag{2.6b}$$
$$C_-(Z) = \frac{\sin\theta}{\sqrt{2}}\varphi_1(Z) + \frac{1}{\sqrt{2}}\varphi_2(Z) + \frac{\cos\theta}{\sqrt{2}}\varphi_3(Z). \tag{2.6c}$$

The optical STIRAP technique is based on the zero-eigenvalue of the dark vector $C_0(Z)$, which is a coherent superposition of the initial optical fields $\varphi_1(z)$ to the final optical fields $\varphi_3(z)$ only. When the coupling order is counterintuitive, it means that the optical fields $\psi_3(z)$ and $\psi_4(z)$ are first coupled, and the coupling between $\psi_1(z)$ and $\psi_3(z)$ is introduced at a later point:

$$\lim_{z\to 0}\frac{\Omega_p(z)}{\Omega_s(z)} = 0, \quad \lim_{z\to L}\frac{\Omega_s(z)}{\Omega_p(z)} = \infty. \tag{2.7}$$

During the conversion, the mixing angle $\theta(z)$ rotates from $\theta(z = 0) = 0$ to $\theta(z = L) = \pi/2$. When the system can be forced to stay in the dark vector during all conversion processes, all of the optical power will be transferred from $\varphi_1(z)$ to $\varphi_3(z)$ without ever going through $\varphi_2(z)$. In order to ensure the adiabatic evolution, the coupling between each pair of adiabatic vectors must be negligible compared with the difference between the energies of these states, so the adiabatic condition is

$$\left|\left\langle\frac{d}{dz}C_0(Z)\,\middle|\,C_\pm(Z)\right\rangle\right| \ll |\varepsilon_0 - \varepsilon_\pm|\,. \tag{2.8}$$

The adiabaticity condition simplifies and becomes $|d\theta/dz| \ll \sqrt{\Omega_p^2 + \Omega_s^2}$; this requires the changes of the coupling coefficients to be very gradual [10].

When the adiabatic limit or perfect phase-matching condition can't be satisfied, the analysis is more difficult. Next we develop a method in which the cascaded conversion processes can be mapped uniquely to an associated three-wave mixing process. After solving the coupling wave equations of the three-wave mixing process, we immediately find the solutions of the corresponding cascaded coupled equations.

III. OPTICAL BLOCH EQUATIONS FOR DIFFERENCE FREQUENCY GENERATION

A. Theoretical model

Comparing the undepleted pump approximation of the DFG process and the dynamics of a two-level atomic system, it has been found that the equations possess the same forms [13,14]. Moreover, the coupled equations for complex-valued amplitudes can be recast as three coupled equations for real-valued variables; the result is the optical Bloch equation.

Under the undepleted pump approximation, the DFG coupled equations can be simplified as [14]

$$i\frac{d}{dt}\begin{bmatrix} A_1(z) \\ A_3(z) \end{bmatrix} = \frac{1}{2}\begin{bmatrix} -\Delta k(z) & 2|q| \\ 2|q| & \Delta k(z) \end{bmatrix}\begin{bmatrix} A_1(z) \\ A_3(z) \end{bmatrix}. \quad (3.1)$$

By using rotation transformation, we can obtain the dressed fields (adiabatic amplitudes):

$$i\frac{d}{dz}\begin{bmatrix} \tilde{A}_1(z) \\ \tilde{A}_3(z) \end{bmatrix} = \frac{1}{2}\begin{bmatrix} -\Omega(z) & -i2\dot{\theta}(z) \\ i2\dot{\theta}(z) & \Omega(z) \end{bmatrix}\begin{bmatrix} \tilde{A}_1(z) \\ \tilde{A}_3(z) \end{bmatrix}. \quad (3.2)$$

The adiabaticity condition for Eq. (3.2) is $|\dot{\theta}| \ll \Omega$, where $q(z) = 2\pi\omega_1\omega_3 d_{\text{eff}} A_2/\sqrt{k_1 k_3}c^2$, $\tan\theta(z) = 2|q|/\Delta k(z)$, and $\Omega(z) = 0.5^*\sqrt{\Delta k^2(z) + 4|q|^2}$; the overdot indicates a space derivative. The two complex-valued amplitudes can be recast as three coupled equations for real-valued variables [15–17]. We now define the new unit vector $B(z) = [u(z), v(z), w(z)]^T$, and the components of this vector are $u(z) = 2\text{Re}(A_1 A_3^*)$, $v(z) = 2\text{Im}(A_1 A_3^*)$, and $w(z) = |A_1|^2 - |A_3|^2$.

The final result is the optical Bloch equation:

$$i\frac{d}{dz}B(z) = \begin{bmatrix} 0 & -\Omega_1 & 0 \\ \Omega_1 & 0 & -\Omega_2 \\ 0 & \Omega_2 & 0 \end{bmatrix} B(z). \quad (3.3)$$

Here, $\Omega_1 = \Delta k(z)$ and $\Omega_2 = 2|q|$. After replacing the amplitudes $v(z)$ and $w(z)$ by the amplitudes $\tilde{v}(z) = iv(z)$ and $\tilde{u}(z) = -u(z)$, and exchanging the places of $w(z)$ and $u(z)$, the Bloch equation takes the form [17]

$$i\frac{d}{dz}\begin{bmatrix} w \\ \tilde{v} \\ \tilde{u} \end{bmatrix} = \begin{bmatrix} 0 & \Omega_2 & 0 \\ \Omega_2 & 0 & \Omega_1 \\ 0 & \Omega_1 & 0 \end{bmatrix}\begin{bmatrix} w \\ \tilde{v} \\ \tilde{u} \end{bmatrix}. \quad (3.4)$$

Equation (3.4) is exactly of the form of Eq. (2.2), when we set $M_\Delta(z) = 0$, $\Omega_1 = \Omega_s$, and $\Omega_2 = \Omega_p$.

The optical field amplitudes $\varphi(z)$ of the two STWM processes are related to the DFG process amplitudes A(z) by [15,16]

$$\varphi_1(z) = |A_1|^2 - |A_3|^2, \quad \varphi_2(z) = 2i\text{Im}A_1 A_3^*,$$
$$\varphi_3(z) = -2\text{Re}A_1 A_3^*, \quad (3.5)$$

and to the adiabatic amplitudes $\tilde{A}(z)$ by [15,16]

$$\varphi_1(z) = (|\tilde{A}_1(z)|^2 - |\tilde{A}_3(z)|^2)\cos\theta(z) + 2\text{Re}[\tilde{A}_1(z)\tilde{A}_3^*(z)]\sin\theta(z), \quad (3.6a)$$
$$\varphi_2(z) = -2\text{iIm}[\tilde{A}_1(z)\tilde{A}_3^*(z)], \quad (3.6b)$$
$$\varphi_3(z) = 2\text{Re}[\tilde{A}_1(z)\tilde{A}_3^*(z)]\cos\theta(z) - (|\tilde{A}_1(z)|^2 - |\tilde{A}_3(z)|^2)\sin\theta(z), \quad (3.6c)$$

These relations hold for any coupling order. When we have solved the adiabatic DFG functions (3.2), we immediately found the solutions to the corresponding two STWM coupled equations (2.2). Such a one-to-one relation between the solutions holds only for restricted sets of initial conditions.

Because the DFG optical field starts at pump field A_1 and goes to signal field A_3 at the end, the initial conditions are the normalized intensities $|A_1(z=0)|^2 = 1$ and $|A_3(z=0)|^2 = 0$. Now we define the two nonlinear coupling coefficients as follows:

$$\Omega_1(z) = \Omega_0(z)\cos(\pi z/2L), \quad \Omega_2(z) = \Omega_0(z)\sin(\pi z/2L). \quad (3.7)$$

It can be easily seen that for all propagation processes the amplitude Ω stays constant ($\Omega = \Omega_0$); its behavior is shown in Fig. 2(a). When the adiabatic condition $|\dot{\theta}| \ll \Omega$ is maintained, the adiabatic solutions for counterintuitive coupling are exactly given by

$$\varphi_1(z) = \{1 - \theta'^2[1 - \cos(z\eta)]/\eta^2\}\cos\theta + [\theta'\sin z\eta/\eta]\sin\theta, \quad (3.8a)$$
$$\varphi_2(z) = \Omega_0\theta'\sin^2(z\eta/2)/\eta^2, \quad (3.8b)$$
$$\varphi_3(z) = [\theta'\sin z\eta/\eta]\cos\theta + \{\theta'^2[1 - \cos(z\eta)]/\eta^2 - 1\}\sin\theta, \quad (3.8c)$$

where $\eta = \sqrt{(\Omega_0^2/4) + \theta'^2}$. It is more difficult to achieve analytic evolution for the two STWM equations (2.2). A useful feature of this model is that it allows a simple analytic solution not only for the final wave energy but also for its spatial evolution.

B. Numerical simulation under ideal conditions

As an example, we considered the four wavelengths is 1.06 μm, 1.31 μm, 4.3 μm, 1.7 μm respectively, and use PPLN crystal which length is 50 mm. The temperature to be set 25 °C in our model. Using the PPLN dispersion relation and neglecting the thermal expansion, the other structural parameters can be calculated from the Sellmeier equation. By numerical integration of Eq. (2.1), Fig. 2(b) shows the normalized intensities of the interacting waves along the nonlinear crystal.

By numerical simulation, we conclude that the final intensities $|\varphi_n(z=L)|^2$ ($n = 1$, 2, and 3) can only depend on the combination $L\Omega_0$. Within the adiabatic limit, $L\Omega_0 \to \infty$, the energies of the optical fields $\varphi_1(z)$ and $\varphi_3(z)$ are exchanged in an expected adiabatic manner; the results are shown in Fig. 2(b). The figure is close to adiabatic, where less than 0.6% of the energy has been transformed into the intermediate wave, and the total energy has been transferred to the final wave. In addition, when the pump intensity is high enough, the intermediate frequency ω_3 is almost never generated. Last, we also show the transfer efficiency as a function of the interaction length L and the interaction amplitude Ω_0, for the special case when Ω_p and Ω_s have equal maximum value; simulation results for Eq. (3.8) are displayed in Fig. 3.

We can see that the energy on the intermediate wave φ_2 oscillates, when $L\Omega_0$ is not very large; In the ideal case, $L\Omega_0 \to \infty$, the energy on the intermediate wave tends to zero, and the energy on the final wave tends to unity. Numerical

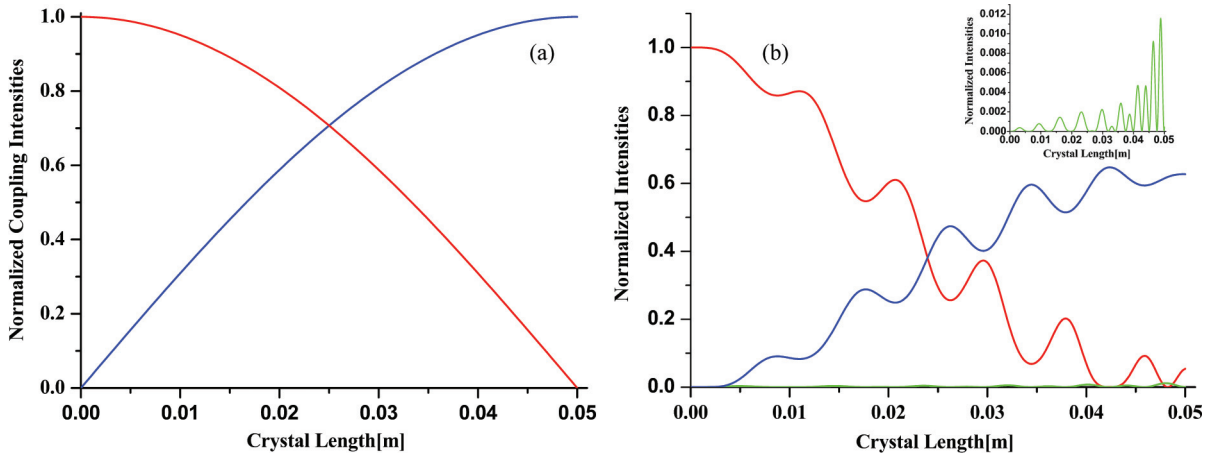

FIG. 2. (Color online) Numerical simulation of the intensities of the interacting waves along the nonlinear medium in the above model. The field intensities are calculated from Eq. (2.1) for $f_1 = 5\sin(\pi z/2L)$ and $f_2 = 5\cos(\pi z/2L)$. (a) Normalized coupling coefficients of the two nonlinear processes. (b) Normalized intensities of the interacting waves with counterintuitive order modulation. The inset shows the intermediate-wave intensity.

modeling results which exhibiting a clear 'STIRAP signature' are shown in Fig. 2. Figure 3 clearly shows the variation tendency of the intermediate optical filed intensity and final conversion efficiency following the change of adiabatic parameter, which could be helpful for us to utilize the STIRAP technology to design the system at the last step.

It is worth pointing out that the effects of the two coupling order are crucial for the perfect phase-matching $\Delta k_1 = \Delta k_2 = 0$ case. By exploring the application of the STIRAP in the realm of frequency conversion, we must consider the realistic situation; the shift of the parameters which affect efficiency of the processes will cause deviation from the condition of perfect phase match, so we must also take into account the effects of the phase mismatch $\Delta k_1 = \Delta k_2 \neq 0$.

IV. EFFECTS OF PHASE MISMATCH TO THE OPTICAL STIRAP

When the condition of perfect phase match cannot be satisfied, the coupled equations in the adiabatic basis (2.6) read as follows [11]:

$$idC(z)/dz = M^{\mathrm{ad}}(z)C(z), \tag{4.1}$$

where

$$M^{\mathrm{ad}}(z) = M_0^{\mathrm{ad}}(z) + M_\Delta^{\mathrm{ad}}(z), \tag{4.2}$$

$$M_0^{\mathrm{ad}}(z) = \begin{bmatrix} \Omega/2 & i\dot{\theta}/\sqrt{2} & 0 \\ -i\dot{\theta}/\sqrt{2} & 0 & -i\dot{\theta}/\sqrt{2} \\ 0 & i\dot{\theta}/\sqrt{2} & -\Omega/2 \end{bmatrix}, \tag{4.3a}$$

$$M_\Delta^{\mathrm{ad}}(z) = \frac{\Delta}{2}\begin{bmatrix} \cos 2\theta/2 & -\sin 2\theta/\sqrt{2} & \cos 2\theta/2 \\ -\sin 2\theta/\sqrt{2} & -\cos 2\theta & -\sin 2\theta/\sqrt{2} \\ \cos 2\theta/2 & -\sin 2\theta/\sqrt{2} & \cos 2\theta/2 \end{bmatrix}. \tag{4.3b}$$

As is shown in Eq. (4.3), the phase mismatching induces nonadiabatic couplings between the dark basis $C_0(Z)$ and the other two adiabatic basis, $C_+(z)$ and $C_-(z)$. The coupling

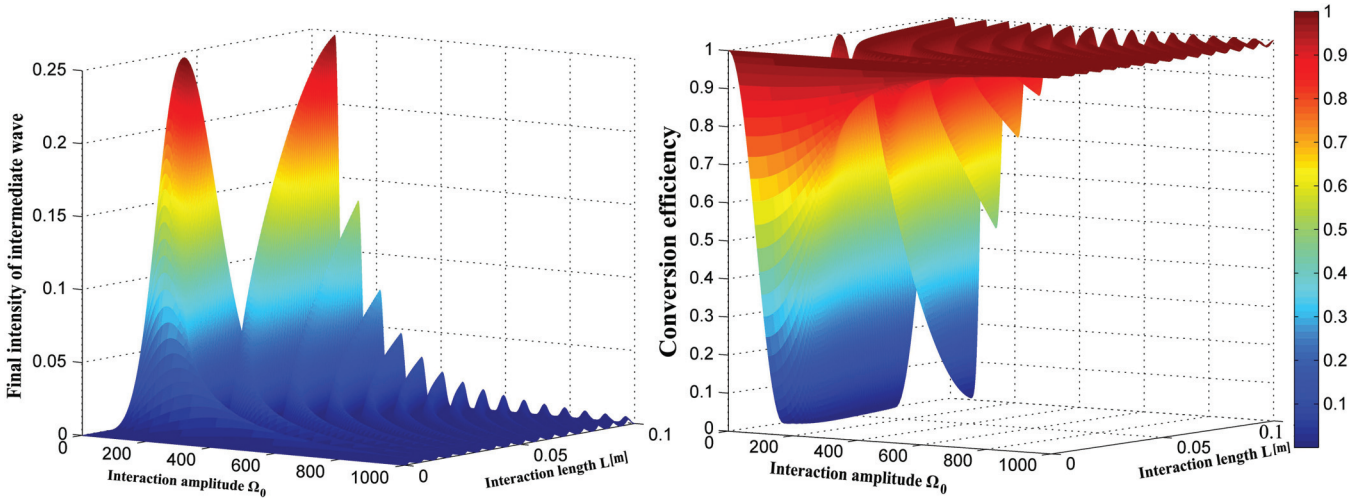

FIG. 3. (Color online) Numerical simulation of the intensities of the interacting waves along the nonlinear medium. (a) Final intensity for the intermediate wave plotted as a function of L and Ω_0. (b) Final conversion efficiency for the final wave plotted as a function of L and Ω_0.

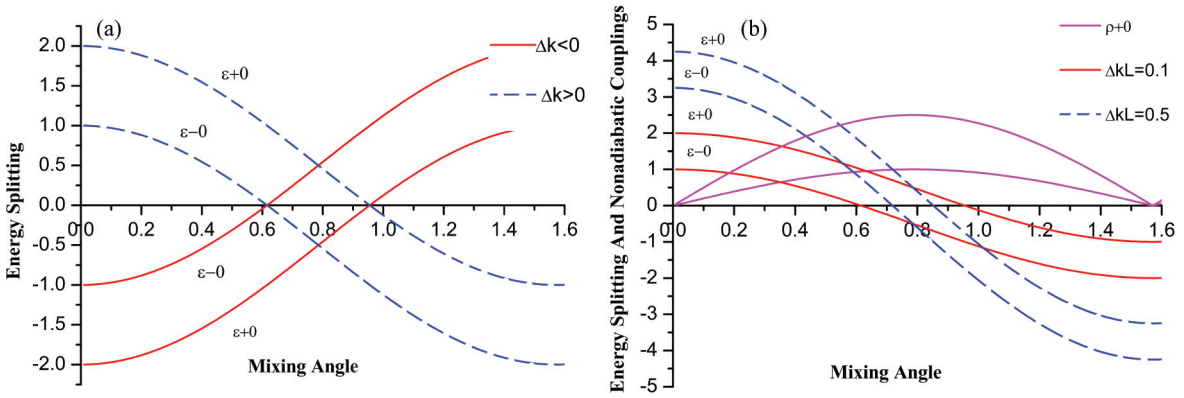

FIG. 4. (Color online) Spatial evolution of the energy splitting ε_{+0} (ε_{-0}) and the nonadiabatic coupling ρ for trigonometric model (3.7). (a) Spatial evolution of energy splitting with different signs of Δk. (b) Evolution of the energy splitting ε_{+0} (ε_{-0}) and the nonadiabatic coupling ρ for different values of $|\Delta k|$.

expression is

$$\rho_{+0}(z) = [2i\dot{\theta}(z) - \Delta \sin 2\theta(z)]/\sqrt{2}, \tag{4.4a}$$

$$\rho_{-0}(z) = \rho_{+0}(z), \tag{4.4b}$$

where $\rho_{+0}(z)$ is the coupling of basis $C_0(z)$ and $C_+(z)$, and $\rho_{-0}(z)$ is the coupling of basis $C_0(z)$ and $C_-(z)$. These couplings will reduce the optical STIRAP conversion efficiency. In addition, the phase mismatching will lead to the energies of all adiabatic basis shifts [11]:

$$\varepsilon_{+0}(z) = [\Omega(z) + 3\Delta \cos 2\theta(z)/2]/2, \tag{4.5a}$$

$$\varepsilon_{-0}(z) = [3\Delta \cos 2\theta(z)/2 - \Omega(z)]/2 \tag{4.5b}$$

where $\varepsilon_{+0} = \varepsilon_+ - \varepsilon_0$ and $\varepsilon_{-0} = \varepsilon_- - \varepsilon_0$, are the energy shifts between the dark basis $C_0(z)$ and the other two adiabatic bases $C_+(z)$ and $C_-(z)$. For $\varepsilon_{+0} = 0$ (or $\varepsilon_{-0} = 0$), it represents the energy as crossing, as illustrated in Fig. 4(a) where the energy splitting is plotted versus the mixing angle. Obviously, no matter whether $\Delta k < 0$ or $\Delta k > 0$, the energy shifts $\varepsilon_{-0}(z)$ and $\varepsilon_{+0}(z)$ always crosses zero. Hence, the energies of basis $C_0(z)$ and $C_-(z)$ or $C_+(z)$ always cross.

As far as STIRAP is concerned, the main loss occurs at the crossings of the adiabatic basis $C_0(z)$ with $C_-(z)$ and $C_+(z)$. When the crossing is close to the maximum of the nonadiabatic couplings [assume the maximum is $\rho(Z_{\max})$], there is a significant nonadiabatic interaction at this crossing and hence a significant energy loss from the dark basis $C_0(z)$ [11,18–20]. So the crossing of the energies with relation to the maxima of the nonadiabatic couplings determines two bounds of phase matching Δ. As is shown in Fig. 4(b), the shifts in $\varepsilon_{-0}(z)$ are larger than those in $\varepsilon_{+0}(z)$. This implies that the crossing in $\varepsilon_{-0}(z)$ is shifted farther from $Z_{\max}$ than that in $\varepsilon_{+0}(z)$, so the main energy losses from the dark basis $C_0(z)$ take place through the crossing in $\varepsilon_{+0}(z)$.

For $\Delta > 0$, the place of crossing in the $\varepsilon_{+0}(z)$ occurs after $Z_{\max}(z_{+0} > Z_{\max})$, and z_{+0} approaches $Z_{\max}$ as Δ increases; consequently, the transfer efficiency approaches zero. In order to simplify the results, we choose the place of the pump couplings Ω_p maxima ($Z_{p\max}$) as a reference point for the crossing place, then

$$\cos 2\theta(z_{p\max}) = -1, \quad \Omega(z_{p\max}) \approx \Omega_p(z_{p\max}). \tag{4.6}$$

From Eq. (4.5a) we can obtain $\Delta = 2\Omega(z)/3$. For $\Delta < 0$, the place of crossing z_{+0} in $\varepsilon_{+0}(z)$ occurs before $Z_{\max}(z_{+0} < Z_{\max})$, and z_{+0} approaches $Z_{\max}$ as $|\Delta|$ increases. We choose $Z_{s\max}$ which is the place of maxima of the Stokes couplings Ω_s as a reference point for the crossing place, then

$$\cos 2\theta(z_{s\max}) = 1, \quad \Omega(z_{s\max}) \approx \Omega_s(z_{s\max}). \tag{4.7}$$

By setting $\varepsilon_{+0} = 0$ from Eq. (4.5a), we can obtain $\Delta = -2\Omega(z)/3$. So the bounds of phase mismatching Δ in optical STIRAP are

$$-2\Omega_s(z)/3 \leqslant \Delta \leqslant 2\Omega_p(z)/3. \tag{4.8}$$

Hence, the phase mismatching width is proportional to $\Omega(z)$. For the (3.7) triangle model, $\Omega(z) = \Omega_0(z)$. We show in Fig. 5 the optical STIRAP evolution for different numbers of phase mismatching Δ. In all cases the energy is converted from frequency (ω_1) to frequency (ω_4) in the end in a stepwise manner. The transient generation of the intermediate frequency (ω_3) is enhanced and the transfer efficiency is damped as Δk increases: from $\Delta kL = 0$ without significant generation of the intermediate frequency (ω_3) to $\Delta kL = 1.5$ with oscillates for the output wave. So the above conclusions are confirmed

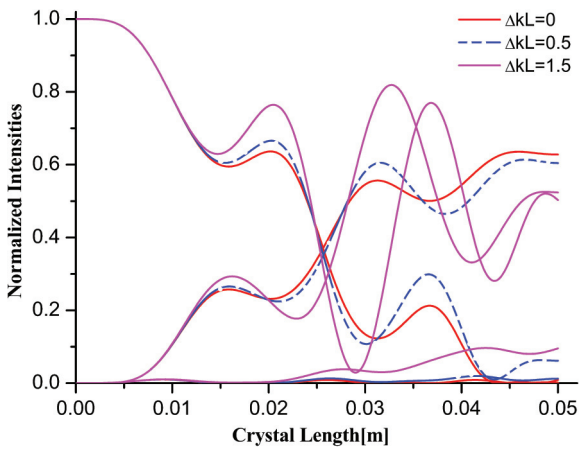

FIG. 5. (Color online) Numerical simulation of the normalized intensities of the interacting waves along the nonlinear medium with different numbers of phase mismatching Δ, with amplitude $\Omega_0 = 40$, under ideal conditions.

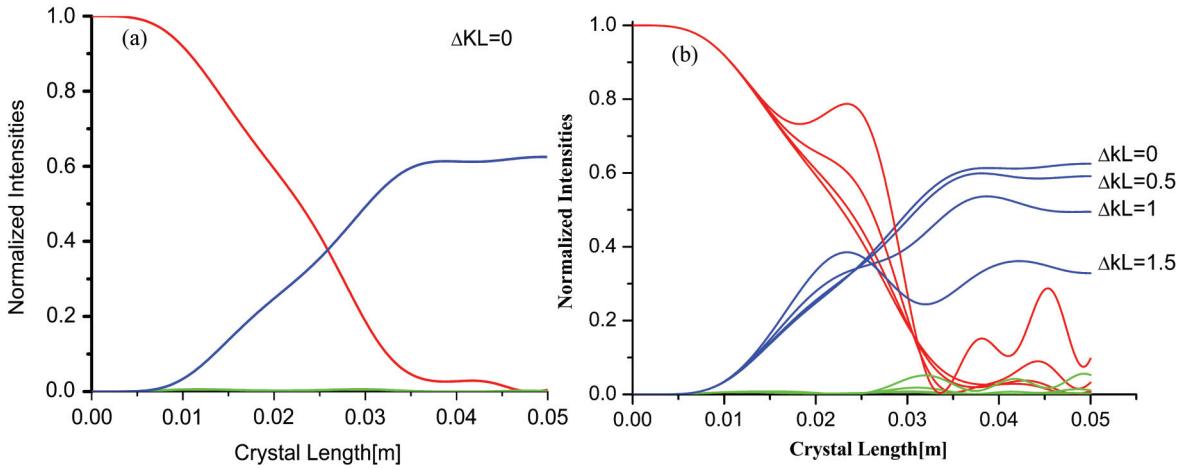

FIG. 6. (Color online) Numerical simulation of the intensities of the interacting waves along the nonlinear medium with the phase-reversal quasi-phase-matching technique. The field intensities are calculated from Eq. (2.1). (a) Phase-matching results. (b) Final conversion efficiency for Δk having different values.

completely, and the analytic bounds are seen to describe the conversion region very accurately. We note that although the example in Fig. 4 uses a trigonometric model, the analysis method is equally suitable for nonlinear coupling coefficients of Gaussian modulation or any other shape.

V. NUMERICAL SIMULATION OF OPTICAL STIRAP IN A NONPERIODIC OPTICAL SUPERLATTICE

At the end of the section we briefly discuss the use of nonperiodic optical superlattice for the generation of optical STIRAP in a cascaded parametric oscillator. To achieve this purpose, both processes were phase matched and the coupling coefficients were modulated as desired. Porat and Arie [10] propose using a phase-reversal quasi-phase-matching technique. For example, we can construct a product of two binary functions as follows:

$$G(z) = \mathrm{sgn}\left[\sin\left(\frac{2\pi}{\Lambda_1}z + \frac{\pi}{\Lambda_1}l_2\right) - \sin\left(\frac{\pi}{\Lambda_1}l_2\right)\right] \times \mathrm{sgn}\left[\sin\left(\frac{2\pi}{\Lambda_2}z + \frac{\pi}{\Lambda_2}l_2'\right) - \sin\left(\frac{\pi}{\Lambda_2}l_2'\right)\right], \quad (5.1)$$

where $\Lambda_1 = l_1 + l_2$, $\Lambda_2 = l_1' + l_2'$ is the period, $l_1(l_1')$ is the length of the positive domains, and $l_2(l_2')$ is the length of the inverted domains. Using simple Fourier analysis yields

$$G_{\mathrm{QPM}}(z) \approx \frac{1}{\pi}(2D_2 - 1)\sin(2\pi D_1)\exp(\pm i\Delta k_1) + \frac{1}{\pi}(2D_1 - 1)\sin(2\pi D_2)\exp(\pm i\Delta k_2), \quad (5.2)$$

Where $D_i = l_1/\Lambda_i$ is the duty cycle. This is the modulation of the second-order nonlinear coefficient $\chi^{(2)}$. If we choose $\Lambda_1 = \Delta k_1$ and $\Lambda_2 = \Delta k_2$, and only keep phase-matched terms, then

$$f_1 = (2D_2 - 1)\sin(2\pi D_1), \text{ and } f_2 = (2D_1 - 1)\sin(2\pi D_2).$$

D_1 and D_2 determine the magnitude of the effective coupling coefficient for each process. Varying the two duty cycles along the crystal achieves the required modulation. The simulation results are presented in Fig. 6(a); good correspondence is obtained with the ideal case results. We also explored the conversion evolution for different numbers of phase mismatching Δ. Simulation results are depicted in Fig. 6(b). Obviously, for $\Delta kL \geqslant 1.5$, the transient generation of the intermediate frequency (ω_3) is significant, and the output wave shows strong oscillation. In order to use phase-reversal quasi-phase-matching for phase matching and coefficient modulation, here we do not take into consideration technological restrictions. Actually, the adiabaticity condition requires the changes of the coupling coefficients to be very gradual, which means a domain lengths need to be as small as possible; otherwise, the intermediate frequency (ω_3) would be generated obviously. This has been discussed in detail in Ref. [10].

It is worth pointing out that the effects of the two coupling order are crucial for the perfect phase-matching $\Delta k_1 = \Delta k_2 = 0$ case, but are not required for large phase mismatch. By analogy with the adiabatic elimination procedure, it can also directly generate frequency φ_4 from frequency φ_1 assuming that both of the DFG processes exhibit a very large phase mismatch but their sum is rather small. This approximation has been discussed in Ref. [9], but due to inherently large phase mismatches, high conversion efficiency was difficult to achieve.

VI. CONCLUSION

In this paper, we have shown that the cascaded wavelength conversion process in the undepleted pump approximation can be mathematically formulated and geometrically visualized in complete analogy with the framework of atomic STIRAP. We have developed an approximate analytical trigonometric model to describe two STWM processes, which are based on the adiabatic DFG process, wherein the pump amplitude is assumed constant along the nonlinear crystal. This model holds the advantage that it does allow a complete solution. The trigonometric model, which is analytically solvable, enables us to show explicitly that, as the adiabaticity increases, the conversion efficiency for the counterintuitive coupling sequence

approaches unity, while it oscillates for the nonadiabatic transition. By analyzing the achieved adiabatic evolution, we were able to derive surprisingly simple and accurate bounds of the high-conversion efficiency region and simple estimates of the adiabatic parameters' magnitude.

Moreover, we also take into account the effects of the phase mismatch to the optical STIRAP technique. By analyzing the emerging adiabatic basis crossings and the positions of the nonadiabatic couplings, we were able to derive simple and accurate bounds of the high-conversion efficiency region and estimates of the width of the phase mismatching. We point out that other approaches (e.g., those based on coherence length maps [21] for the involved nonlinear processes) are also useful to analysis the effects of the phase mismatch, but the analysis processes were too complicated to be of use here. Finally, a technologically feasible method for carrying out such a process was proposed and numerically demonstrated to be effective.

The results in this paper also have potential significance in applications of STIRAP where the two couplings, pump and Stokes, are of different physical natures, such as in the DFG process wherein the Stokes coupling is replaced by phase mismatching ΔK. Suitably extended, we here draw upon a mathematical equivalence of the STIRAP STWM processes with an adiabatic DFG process to suggest a potentially useful technique, DFG-STIRAP, which may allow the complete transfer of energy from one wavelength to another in a single three-wave mixing process.

ACKNOWLEDGMENTS

This work was cofunded by the Key Program of the Natural Science Foundation of Guangdong Province (Grants No. 10251063101000001 and No. 8251063101000006) and the National Natural Science Foundation of China (Grant No. 60878063).

[1] Robert Clelia, Michau Vincent, and Fleury Bruno, Opt. Express **20**, 15636 (2012).
[2] Tsutomu Yanagawa, Osamu Tadanaga, Katsuaki Magari, Yoshiki Nishida, Hiroshi Miyazawa, Masaki Asobe, and Hiroyuki Suzuki, Appl. Phys. Lett. **89**, 221115 (2006).
[3] Kalyan V. Bhupathiraju, Joseph D. Rowley, and Feruz Ganikhanov, Appl. Phys. Lett. **95**, 081111 (2009).
[4] Jianhua Chang, Qinghe Mao, and Sujuan Feng, Opt. Lett. **35**, 3486 (2010).
[5] Y. S. Kivshar, A. A. Sukhoruukov, and S. M. Saltiel, Phys. Rev. E **60**, R5056 (1999).
[6] T. Ellenbogen, A. Arie, and S. M. Saltiel, Opt. Lett. **32**, 262 (2007).
[7] Jeffrey Moses, Haim Suchowski, and Franz X. Kärtner, Opt. Lett. **37**, 1589 (2012).
[8] Nikolay V. Vitanov, Thomas Halfmann, Bruce W. Shore, and Klaas Bergmann, Annu. Rev. Phys. Chem. **52**,763 (2001).
[9] Gil Porat, Yaron Silberberg, Ady Arie, and Haim Suchowski, Opt. Express **20**, 3613 (2012).
[10] Gil Porat and Ady Arie, J. Opt. Soc. Am. B **29**, 2901 (2012).
[11] Iavor I. Boradjiev and Nikolay V. Vitanov, Phys. Rev. A **81**, 053415 (2010).
[12] A. A. Rangelov and N. V. Vitanov, Phys. Rev. A **85**, 045804 (2012).
[13] H. Suchowski, D. Oron, A. Arie, and Y. Silberberg, Phys. Rev. A **78**, 063821 (2008).
[14] Ren Liqing, Li Yongfang, Li Baihong, Wang Lei, and Wang Zhaohua, Opt. Express **18**, 20428 (2010).
[15] N. V. Vitanov and S. Stenholm, Phys. Rev. A **55**, 648 (1997).
[16] Timo A. Laine and Stig Stenholm, Phys. Rev. A **53**, 2501 (1996).
[17] N. V. Vitanov and B. W. Shore, Phys. Rev. A **73**, 053402 (2006).
[18] P. A. Ivanov, N. V. Vitanov, and K. Bergmann, Phys. Rev. A **70**, 063409 (2004).
[19] M. V. Danileiko, V. I. Romanenko, and L. P. Yatsenko, Opt. Commun. **109**, 462 (1994).
[20] G. G. Grigoryan and Y. T. Pashayan, Opt. Commun. **198**, 107 (2001).
[21] C. Altucci, R. Bruzzese, C. de Lisio, M. Nisoli, E. Priori, S. Stagira, M. Pascolini, L. Poletto, P. Villoresi, V. Tosa, and K. Midorikawa, Phys. Rev. A **68**, 033806 (2003).